Research Square

Preprints are preliminary reports that have not undergone peer review.
They should not be considered conclusive, used to inform clinical practice,
or referenced by the media as validated information.

SiFEA4 encoding the bZIP transcription factor regulates panicle architecture in foxtail millet (Setaria italica)

Tianguo Wang
Shanxi Agricultural University
Lu Chen
Shanxi Agricultural University
Shujie Dai
Shanxi Agricultural University
Shangkun Niu
Shanxi Agricultural University
Yanyu Yang
Shanxi Agricultural University
Yuqin Zhao
Shanxi Agricultural University
Shiyuan Wang
Shanxi Agricultural University
Yixuan Ma
Shanxi Agricultural University
Lejie Yang
Shanxi Agricultural University
Kai Zhao
Shanxi Agricultural University
Xiaorui Li
Shanxi Agricultural University
Shuqi Dong
Shanxi Agricultural University
Hongzhi Wang
Shanxi Agricultural University
Xiaoqian Chu
Shanxi Agricultural University
Xiangyang Yuan
Shanxi Agricultural University
Jiagang Wang

Shanxi Agricultural University

Lulu Gao

Shanxi Agricultural University

Guanghui Yang

yanggh1991@163.com

Shanxi Agricultural University

Research Article

Keywords: foxtail millet (Setaria italica), panicle apex branching, SiFEA4, panicle architecture, inflorescence development

Posted Date: August 13th, 2026

DOI: https://doi.org/10.21203/rs.3.rs-10443975/v1

License: This work is licensed under a Creative Commons Attribution 4.0 International License. Read Full License

Additional Declarations: No competing interests reported.

Abstract

Panicle architecture was a key factor determining the crop yield. Panicle developed from the inflorescence meristem (IM), whose size and activity influenced the final morphological structure of the panicle. In this study, a foxtail millet landrace WY159 showing the phenotype of panicle apex branching was identified, which might be caused by abnormal differentiation of IM. Through map-based cloning, the candidate gene Seita.4G118000 (designated SiFEA4) encoding a bZIP transcription factor was isolated. Compared with the variety Yugu1 with normal panicle development, there was a 2649 bp deletion in the promoter region of SiFEA4 in WY159, which leaded to a significant downregulation of its expression. Furthermore, using the CRISPR/Cas9 gene editing technology, two homozygous SiFEA4 knockout mutants were obtained. Compared with the wild-type Ci846, the SiFEA4 knockout mutant showed an enlarged, flattened and then centrally depressed IM, ultimately resulting in the panicle apex branching phenotype. Meanwhile, the SiFEA4 gene knockout mutant also exhibited the decreased plant height, increased number of panicle primary branches, and slender panicle primary branches. In addition, RNA-seq analysis revealed that SiFEA4 regulated panicle development likely through the plant hormone signaling pathway. By integrating DAP-seq and RNA-seq analyses, 89 potential direct downstream target genes of SiFEA4 were identified, including SiERF109, SiCDF1, SiPL3, and SiAGL61, which are related to inflorescence development. In summary, this study revealed the important role of SiFEA4 in regulating panicle architecture, providing a new insight into the genetic regulatory mechanism of inflorescence development in foxtail millet.

Introduction

Foxtail millet (*Setaria italica*), an ancient cereal crop domesticated approximately 10,000 years ago, served as a vital food source in many arid and semi-arid regions due to its drought resistance, tolerance to poor soils, and high water-use efficiency (Yang et al., 2012; Vidhya et al., 2023; Bettinger et al., 2010). The panicle, which was the reproductive organ and a principal determinant of yield formation in cereal crops such as foxtail millet, rice (*Oryza sativa*), and oat (*Avena sativa*), originated from the inflorescence meristem (IM), a population of cells with stem cell characteristics that differentiated from the shoot apical meristem (SAM) during the reproductive growth phase. The IM was responsible for initiating branch meristems (BMs) or directly forming spikelet meristems (SMs). The size and activity of IM profoundly affected the number of spikelets and ultimately determined the grain yield (Wang et al., 2021; Tanaka et al., 2013).

Panicle development was a complex biological process regulated by environmental factors and multi-layered genetic regulations. Recent advances in molecular biology and genomic technologies have facilitated the cloning of a series of key genes involved in panicle development, which participated in processes such as maintaining and transitioning apical meristems, developing the IM, forming SMs, and regulating floral organogenesis. Furthermore, these genes were integrated into multiple regulatory pathways, including small peptide-receptor signaling pathway, G-protein mediated signaling

pathway, plant hormone signaling pathway, photoperiod signal pathway, transcription factor regulatory network, and microRNA-target modules (Wang et al., 2021).

The classic CLAVATA-WUSCHEL (CLV-WUS) negative feedback pathway represented a core regulatory mechanism for maintaining stem cell homeostasis in the SAM of plants, first discovered in *Arabidopsis* (*Arabidopsis thaliana*). *WUS*, a homeodomain transcription factor expressed in the organizing center of the SAM, directly activated the transcription of *CLAVATA3* (*CLV3*), a key stem cell marker gene. CLV3was a small peptide signaling molecule, that feedback inhibited the expression of *WUS* through the leucine-rich repeat (LRR) kinase receptor complex CLAVATA1/CLAVATA2 (CLV1/CLV2), thereby forming a negative feedback loop for stem cell homeostasis. Mutation in *CLV1*, *CLV2*, or *CLV3* resulted in the enlarged IM, leading to the increased number of floral organs (Brand et al., 2000; Schoof et al., 2000; Clark et al., 1997; Fletcher et al., 1999; Jeong et al., 1999). Subsequently, the similar regulatory networks have been identified in crops such as maize (*Zea mays*) and rice. In maize, *THICK TASSEL DWARF1* (*TD1*) was the ortholog of *CLV1*, *FASCIATED EAR2* (*FEA2*) was the ortholog of *CLV2*, and *ZmCLE7* and *ZmCLE14* were homologs of *CLV3*. Loss-of-function mutants of these genes exhibited the enlarged IM, producing more axillary meristems (AMs), which consequently leaded to the fasciated ear, and some mutants also displayed the apex branching ear (Bommert et al., 2005; Taguchi-Shiobara et al., 2001; Je et al., 2018). *FASCIATED EAR3* (*FEA3*), the maize *CLV* receptor sharing sequence similarity with *FEA2*, had been integrated into the CLV-WUS feedback regulation model. The *fea3* mutant also showed an enlarged IM and fasciated ear phenotype (Je et al., 2016). In rice, *FLORAL ORGAN NUMBER1* (*FON1*) and *FON2/FON4* were orthologs of *CLV1* and *CLV3*, respectively. Genetic analyse indicated that *FON1* and *FON2/FON4* played significant roles in regulating SAM size, IM activity, and floral meristems (FMs) formation in rice (Chu et al., 2006; Suzaki et al., 2006; Suzaki et al., 2004).

The TGA transcription factors, which belonged to the subgroup D of the basic leucine zipper (bZIP) family, could recognize the core cis-regulatory element TGACG and have been shown to play crucial regulatory roles in panicle development. In *Arabidopsis*, *PERIANTHIA* (*PAN*), encoding a TGA transcription factor, primarily expressed in FMs and early floral primordia, and involved in regulating floral organs number and arrangement. The *pan* mutant exhibited enlarged SAM, increased number of floral organs (particularly sepals and petals), and abnormal organ arrangement (Maier et al., 2011; Running et al., 1996; Chuang et al., 1999). The maize bZIP transcription factor *FASCIATED EAR4* (*FEA4*) was the homolog of *PAN* and its expression persisted throughout all stages of IM development. Mutation in *FEA4* resulted in the semi-dwarfism phenotype, accompanied by multiple phenotypic alterations, including fasciated and shorter ear, abnormal tassel spikelets, increased kernel row number (KRN), and enlarged vegetative and inflorescence tissue. *FEA4*promoted meristem differentiation by regulating genes involved in auxin response and leaf differentiation and polarity. The increased KRN in *fea4* mutant had an important potential application for increasing crop yield (Pautler et al., 2015). In barley (*Hordeum vulgare*), *HvFEA4* was the ortholog of maize *FEA4*, with its highest expression during the initial stage of IM development. *HvFEA4* ensured subsequent normal development and maintained yield-related traits such as spikelet number by

restricting the excessiveproliferation of IM. Loss-of-function mutant *hvfea4* displayed the enlarged IM, shorter spike, smaller grains, and the production of additional spikelets. *HvFEA4* participated in targeting multiple pathways during inflorescence development, including transcriptional activity, plant hormone signaling pathway, and redox status regulation (Wang et al., 2023). In rice, *OsbZIP47* was the homolog of *PAN* and *FEA4*. The changes in plant height and SAM of the *osbzip47*mutant showed a similar trend to those observed in the *fea4* mutant. Additionally, the *osbzip47*mutant showed the delayed flowering, increased stamen numbers, chimeric floral organs, and larger grains (Prakash et al., 2022).

Panicle apex branching in foxtail millet, commonly referred to as the “cat’s claw” phenotype, was a type of the panicle architecture. Zhu et al. (2021) reported that SvFON2, homologous to the small peptide CLV3and FON2, regulated panicle apex branching in green foxtail (*Setaria viridis*), the ancestral specie of foxtail millet. However, the genetic regulator of panicle apex branching in foxtail millet remained elusive. In this study, we identified the bZIP transcription factor *SiFEA4* controlling panicle apical branching in foxtail millet through map-based cloning and gene knockout validation. In addition, *SiFEA4* also affected phenotypes such as plant height, IM size and the number and structure of panicle primary branches. Furthermore, the regulatory network of *SiFEA4* was initially revealed through RNA sequencing (RNA-seq) and DNA affinity purification sequencing (DAP-seq). Thus, this study provided an new insight into understanding the genetic regulation of panicle architecture development in foxtail millet, offering a theoretical foundation and gene resources for future improvement of panicle architecture and yield through molecular breeding.

Materials and methods

Plant materials and growth conditions

Foxtail millet landrace WY159 was obtained from the Chinese Crop Germplasm Information System (https://www.cgris.net/home), with the unified accession number 00004165. The Yugu1 cultivar was an elite foxtail millet variety bred by the Anyang Academy of Agricultural Sciences in Henan Province, China, and served as the reference genome accession for foxtail millet (Bennetzen et al., 2012). The *SiFEA4* knockout lines *sifea4-8* and *sifea4-9* were both derived from the Ci846 (wild type), which exhibited relatively high genetic transformation efficiency. All experimental materials were grown in the Shenfeng Experimental Field of Shanxi Agricultural University or under greenhouse conditions with a photoperiod of 10 hours of light and 14 hours dark.

Phenotype investigation and data statistical analysis

Young panicles or inflorescence meristems (IMs) of WY159, Yugu1, Ci846, *sifea4-8*, and *sifea4-9* were observed and photographed using a Leica Ivesta 3 stereomicroscope (Leica Microsystems, Germany). After photographing, the height and width of IMs were measured using ImageJ software, with at least five plants per variety (line). For Ci846, *sifea4-8*, and *sifea4-9*, the plants and panicle-related traits at mature stage were investigated, including the plant height, the main panicle length, the main panicle diameter, the main panicle weight, the number of panicle primary branches, the length of panicle primary

branches, the width of panicle primary branches, the number of grains per panicle primary branch, the grain length, the grain width, and the 1000-grain weight. Among these, the main panicle diameter was measured at the thickest part of the main panicle; the length and width of panicle primary branches and the number of grains per panicle primary branch were measured using three panicle primary branches from the middle part of the main panicle, with at least eight plants per variety (line). Grain-related traits were measured using an SC-G automatic seed tester (WSeen, China), with no fewer than 250 grains per measurement each time and at least eight plants per variety (line). All datas were statistically analyzed using Excel, and visualization were performed using GraphPad Prism 9.5.0 software. P-values were calculated using the Student's t-test.

Construction of mapping population and map-based cloning

WY159 (female parent) and Yugu1 (male parent) were crossed in the spring of 2022 at the Shenfeng Experimental Field of Shanxi Agricultural University. The seeds harvested were grown in a greenhouse in the same year, and true F_1 hybrids were identified via morphological markers and Simple Sequence Repeat (SSR) molecular markers. F_1 plants were self-pollinated to produce F_2 seeds, which were sown in May 2023 at the Shenfeng Experimental Field of Shanxi Agricultural University to generate the F_2 segregating population. For the fine mapping population, the F_2 individual plants were first genotyped using the *InDel48* and *InDel56* markers flanking the preliminary mapping candidate interval. Seeds from the heterozygous genotypic individuals were sown to obtain the $F_{2:3}$ population, from which 332 recessive individuals were identified. For map-based cloning, Bulked Segregant Analysis (BSA) was adopted, combined with SSR, Insertion-Deletion (InDel), and STARP molecular markers for linkage marker screening and genotyping of the recessive population. The mapping interval was determined by calculating the number of recombinants in recessive individuals. Details of the relevant molecular markers were provided in Table S1.

Phylogenetic tree analysis

The protein sequence of *SiFEA4* was used as a query to perform a BLAST search against the reference genomes of *Arabidopsis thaliana* (*Arabidopsis thaliana* TAIR10), maize (*Zea mays* RefGen_V4), rice (*Oryza sativa* v7.0), barley (*Hordeum vulgare* r1), and foxtail millet (*Setaria italica* v2.2) in the Phytozome database (https://phytozome-next.jgi.doe.gov/). The top 30 hits were selected for phylogenetic analysis. Multiple sequence alignment of these protein sequences was carried out using the ClustalW algorithm implemented in MEGA11 software. Phylogenetic tree was subsequently constructed based on the Neighbor-Joining method. The reliability of the tree topology was assessed using the bootstrap method with 1000 replications. The protein sequences of these 30 hits were provided in Table S2.

Protein subcellular localization

The coding sequence (CDS) of *SiFEA4* without the stop codon was amplified from Yugu1 and cloned into the *p35S:MCS-EGFP* vector to generate the fusion construct *p35S:SiFEA4-EGFP*. The fusion construct was introduced into *Agrobacterium tumefaciens* strain GV3101 using the freeze-thaw method and

injected into the leaf epidermal cells of *Nicotiana benthamiana* for transient expression, with the empty vector used as a control. GFP fluorescence signals in the tobacco epidermal cells were observed 72 hours after injection using an MD3000 LED (Leica) fluorescence microscope. Details of the relevant primers were provided in Table S3.

RNA extraction and quantitative real-time PCR (qRT-PCR)

To investigate whether the expression level of *SiFEA4* differed between Yugu1 and WY159, total RNA was extracted from young panicles (1-2 cm) of both varieties, following the method previously described by Zepeda et al. (2022). Complementary DNA (cDNA) was synthesized from the extracted RNA using the StarScript Pro All-in-one RT Mix kit from Genstar Biotechnology Co., Ltd. (Beijing, China). qRT-PCR was performed using the 2×RealStar Universal SYBR qPCR Mix kit (Genstar Biotechnology). Three biological replicates were set up, each with three technical replicates. The *Seita.8G043100* (*Actin*) gene was used as the internal reference gene, and relevant primers for qRT-PCR were designed using NCBI Primer-BLAST. For the expression pattern analysis of *SiFEA4*, various tissue samples were collected from Yugu1. RNA extraction, reverse transcription, and expression quantification for these samples were carried out using the methods described above. Details of the relevant primers were provided in Table S3.

Knockout vector construction and plant transformation

To generate the knockout vector of *SiFEA4*, a single-guide RNA (sgRNA) was designed based on the CDS of *SiFEA4*. The *SiFEA4* knockout vector was then constructed following the method described by Xing et al. (2014). Subsequently, the knockout vector was introduced into callus tissues of foxtail millet variety Ci846 via Agrobacterium-mediated transformation to generate *SiFEA4* knockout mutants. The sequence of the sgRNA and the primers for detecting knockout target were provided in Table S3.

RNA-seq library construction and differentially expressed genes (DEGs) analysis

Young panicles (1-2 cm) were respectively collected from Ci846 and *sifea4-8* mutant, with three biological replicates for each line. Each replicate consisted of tissues pooled from at least 10 individual plants. Total RNA was extracted using TRIzol reagent according to the manufacturer's instructions. Transcriptome libraries were then constructed using the VAHTS Universal V10 RNA-seq Library Prep Kit (Premixed Version) following the provided protocol. The libraries were sequenced on an Illumina NovaSeq 6000 platform, generating 150 bp paired-end reads. Raw reads were subjected to quality control using fastQC (version v0.11.9) with default parameters. Adapter-trimming and quality filtering were performed with fastp (version 0.20.1; parameters: --length_required 50) to remove adapter sequences, low-quality reads, and reads shorter than 50bp. The clean reads were aligned to the reference genome (*Setaria italica* v2.2) using HISAT2 (version 2.1.0; parameters: --rna-strandness RF --fr). Gene expression levels were quantified as FPKM, and read counts for each gene were obtained using HTSeq-count (version 0.11.2). DEGs was conducted with DESeq2 (version 1.22.2). Genes meeting the criteria of an adjusted p-value < 0.05 and $|\log_2(\text{fold change})| > 1$ were defined as DEGs.

DNA affinity purification sequencing of *SiFEA4*

A Halo-tag expression plasmid (pFN19K HaloTag® T7 SP6) for the transcription factor was constructed based on the *SiFEA4* CDS sequence. The plasmid was used for in vitro cell-free protein expression employing the TnT® SP6 High-Yield Wheat Germ Protein Expression System (Promega, L3260). Genomic DNA was extracted from seedlings of the Yugu1 variety using the FastPure Plant DNA Isolation Mini Kit (Vazyme, DC104-01). The extracted DNA underwent end repair, A-tailing, and adapter ligation sequentially, followed by bead-based purification to complete the initial library construction. An Input control (the directly prepared gDNA library) was included to verify DNA extraction efficiency and for subsequent DAP efficiency calculations. Magne® HaloTag® Beads (Promega, G7281) were equilibrated by washing four times with Equilibration Buffer at room temperature, aliquoted, and the supernatant was discarded. The in vitro expressed protein solution was mixed with the beads and incubated at 25°C with shaking at 1500 rpm for 1 hour to allow protein-bead binding. The supernatant containing unbound protein was removed, and the beads were washed three times with Equilibration Buffer. A mixture of 25 µl Equilibration Buffer and 25 µl DNA library was added to the beads and incubated at 25°C with shaking at 1500 rpm for 1 hour to facilitate specific binding between the target protein and DNA fragments. The beads were then washed three more times with Equilibration Buffer to remove non-specifically bound DNA. To elute specifically bound DNA, 30 µl of 50 mM Tris-HCl (pH=8.5) was added to the beads, followed by a 10-minute incubation in a metal bath at 98°C. The eluted DNA (supernatant) was stored at -20°C. The KAPA Real-Time Library Amplification Kit (Kapa Biosystems, 7958986001) was used to add index adapters to the eluted DNA via PCR. The product was size-selected and purified using beads to complete the final library amplification (Bartlett et al., 2017). Qualified libraries were sequenced on the Illumina NovaSeq X Plus platform. Raw reads obtained from sequencing were subjected to quality control using fastQC (version 0.11.5) with default parameters. Trimmomatic software (version 0.39) was used to filter the raw reads, removing adapter sequences, low-quality reads, and reads shorter than 20 bp. The high-quality reads were aligned to the reference genome (*Setaria italica* v2.2) using the mem algorithm in BWA software with default parameters. Peak calling was performed using MACS2 software (version 2.2.7.1; parameters: -f BAMPE -q 0.05). motif analysis within the peak regions was conducted using Hypergeometric Optimization of Motif EnRichment (HOMER; version v4.11). DAP-seq tracks showed fusion protein binding sites were visualized using IGV.

Results

Identification and genetic analysis of the panicle apex branching phenotype in foxtail millet

A foxtail millet landrace showing the panicle apex branching phenotype was identified and designated as WY159 (Figure 1a-c). Stereomicroscope observations revealed that, compared to the variety Yugu1 with a normal panicle phenotype, the inflorescence meristem (IM) apex of WY159 exhibited a flattened characteristic at the stage of IM to BM transition (Figure 1d-e), and a distinct branching phenotype was observed at the apex of the young panicle (Figure 1f-g), suggesting that this panicle apex branching phenotype might be associated with abnormal IM development. To understand the genetic basis of the

panicle apex branching in foxtail millet, we performed a cross between WY159 and Yugu1, and all F_1 individual plants displayed a normal panicle phenotype. In the F_2 segregating population, the ratio of individuals with the normal panicle phenotype to those with the panicle apex branching phenotype was 183:48, which conformed to the expected 3:1 Mendelian ratio ($\chi^2 = 2.195$, $p > 0.05$), indicating that the panicle apex branching phenotype was controlled by a single recessive gene.

Map-based cloning of the panicle apex branching gene

To identify the gene responsible for panicle apex branching in foxtail millet, we utilized the aforementioned F_2 segregation population and conducted linkage analysis combined with Bulked Segregant Analysis (BSA) and SSR markers. Markers *p2*, *S233*, and *p89* on chromosome 4 were found to be linked to the phenotype (Figure S1). In order to determine the candidate interval where the target gene was located, we genotyped the 48 recessive individuals in the F_2 population using these three markers and their nearby SSR and InDel markers, and mapped the panicle apex branching gene to the candidate interval between markers *InDel4-52* and *InDel4-55* (Figure 2a). For fine mapping, we genotyped 332 recessive individuals from $F_{2:3}$ population using the InDel and STARP markers between *InDel4-52* and *InDel4-55*. Ultimately, the candidate interval was narrowed down to a ~1.28 Mb physical region (Chr4: 10,914,497-12,198,076 bp) between markers *STARP-2* and *STARP-13* (Figure 2a).

According to the annotation information of the Yugu1 reference genome (*Setaria italica v2.2*) in the Phytozome plant genome database, 50 annotated genes were identified within this candidate interval. Previous studies have shown that bZIP transcription factor family members, such as *FEA4* (*Zm00001d037317*), *HvFEA4* (*HORVU7Hr1G042170*), *OsbZIP47* (*LOC_Os06g15480*), and *PAN* (*AT1G68640*), played crucial regulatory roles in IM development, and the maize *fea4* mutant showed a ear apical branching phenotype (Pautler et al., 2015; Wang et al., 2023; Prakash et al., 2022; Chuang et al., 1999). Among the 50 annotated genes, we found that the gene *Seita.4G118000* encoded a bZIP transcription factor. Phylogenetic analysis revealed that *Seita.4G118000* was homologous to *ZmFEA4*, *OsbZIP47* and *HvFEA4*, with the closest relationship being to *ZmFEA4* (Figure 2b; S2). Consequently, *Seita.4G118000* was named *SiFEA4*. We amplified the *SiFEA4* genomic sequence from WY159 and confirmed it by Sanger sequencing. Sequence analysis revealed that, compared with the Yugu1 reference genome, there was a 2649-bp deletion in the promoter region of this gene in WY159 (Figure 2c). To determine whether this structural variation affected the expression of *SiFEA4*, we examined the expression level of *SiFEA4* in young panicles of Yugu1 and WY159, and found that the relative expression level of *SiFEA4* in WY159 was significantly lower than in Yugu1 (Figure 2d). Based on these findings, we hypothesized that *SiFEA4* might be the target gene regulating the panicle apex branching in foxtail millet.

Expression pattern and protein subcellular localization of *SiFEA4*

To investigate the expression pattern of *SiFEA4*, we performed qRT-PCR to detect its expression levels in various tissues of Yugu1. The results showed that *SiFEA4* was highly expressed in young leaf, young panicle, and grain at 10 days after pollination (10 DAP)(Figure 3a). Elucidating the subcellular

localization of a protein was crucial for understanding its biological function. To this end, we constructed the *p35S:SiFEA4-EGFP* fusion expression vector and transformed it into epidermal cells of tobacco leaves for transient expression via *Agrobacterium*-mediated transformation. Fluorescence microscopy observation revealed that, in contrast to the control *p35S:GFP* where the GFP signal was detected throughout the entire tobacco epidermal cell, the GFP signal of the *p35S:SiFEA4-EGFP* fusion protein was exclusively localized to the nucleus (Figure 3b). This result indicated that *SiFEA4* was a nuclear-localized protein, which was consistent with the predicted function of *SiFEA4* as a transcription factor.

SiFEA4 was a pleiotropic gene that regulated panicle structure and plant height in foxtail millet

To verify the function of *SiFEA4*, we knocked out the *SiFEA4* in the foxtail millet variety Ci846 background using the CRISPR/Cas9 genome-editing system, and two independent homozygous knockout lines (*sifea4-8* and *sifea4-9*) were obtained. In the *sifea4-8* and *sifea4-9* mutant, one adenine (A) and one thymine (T) base was inserted into *SiFEA4*, respectively, resulting in a frameshift mutation and the premature termination of protein translation (Figure 4a). Phenotypic analysis revealed that, compared with Ci846, the IM of *sifea4-8* and *sifea4-9* was significantly enlarged at the early stage of the IM-to-BM transition (Figure 4b, g-h). At the late stage of this transition, the apical region of the IM began to flatten. By the BM-to-SM transition stage, the central part of this flattened region became depressed to form a groove, which eventually developed into a distinct branching phenotype at the apex of the young panicle (Figure 4b-c). These observations verified that *SiFEA4* was the causal gene controlling panicle apex branching in foxtail millet.

In addition, compared with the wild-type Ci846, the plant height of *sifea4-8* and *sifea4-9* was significantly reduced, while the panicle diameter was significantly increased (Figure 4d-e, i and l). Moreover, the number of panicle primary branches significantly increased by 54.29% and 46.57%, respectively, which was attributed to the emergence of extra panicle primary branches on the rachis (Figure 4f and m). In contrast, there were no significant differences in the panicle length, single panicle weight, grain width, grain length and thousand grain weight (Figure 4j-k; S3). Notably, the significantly increased number of panicle primary branches in *sifea4-8* and *sifea4-9* did not lead to an increase in single panicle weight, prompting us to further investigate the traits related to panicle primary branches. We observed that in *sifea4-8* and *sifea4-9*, the length of panicle primary branches increased, the width of panicle primary branches decreased significantly, and the number of grains per panicle primary branch significantly decreased by 40.52% and 42.51%, respectively (Figure 4n-p). The above results indicated that in *sifea4-8* and *sifea4-9*, the significant increase in the number of panicle primary branches was accompanied by a significant decrease in the width of panicle primary branches and the number of grains per panicle primary branch. Taken together, *SiFEA4* was a pleiotropic gene that not only regulated the panicle apical branching phenotype but also participated in controlling plant height and the number and structure of panicle primary branches.

SiFEA4 regulated panicle development likely through the plant hormone signaling pathway.

To explore the transcriptional regulatory network of *SiFEA4*, we performed RNA-seq analysis on 1-2 cm young panicles of Ci846 and *sifea4-8*. A total of 763 DEGs were identified between Ci846 and *sifea4-8*, among which 605 DEGs were downregulated and 158 DEGs were upregulated in *sifea4-8* (Figure 5a-b; Table S4). GO enrichment analysis showed that these DEGs were significantly enriched in multiple biological processes, such as response to jasmonic acid (GO:0009753, p value = 4.50982E-07), response to abscisic acid (GO:0009737, p value = 2.30599E-05), response to salicylic acid (GO:0009751, p value = 5.65864E-05), regulation of jasmonic acid mediated signaling pathway (GO:2000022, p value = 1.67517E-04), response to gibberellin (GO:0009739, p value = 5.36745E-04), negative regulation of gibberellic acid mediated signaling pathway (GO:0009938, p value = 8.09822E-04), ethylene-activated signaling pathway (GO:0009873, p value = 1.49989E-03), response to ethylene (GO:0009723, p value = 3.22523E-03), gibberellin metabolic process (GO:0009685, p value = 5.08369E-03), regulation of salicylic acid biosynthetic process (GO:0080142, p value = 7.52627E-03), ethylene biosynthetic process (GO:0009693, p value = 2.08245E-02), positive regulation of abscisic acid biosynthetic process (GO:0010116, p value = 3.15551E-02), and positive regulation of transcription (GO:0045893, p value = 9.89775E-04), and so on (Figure. 5c; Table S5). These results suggested that *SiFEA4* regulated panicle structure likely through the plant hormone signaling pathway.

Furthermore, we found that among the DEGs, there were multiple genes whose homologous genes in other species have been reported to be related to inflorescence development (Figure 5d). Among these genes, some were downregulated in the *sifea4-8* mutant. For example, *SiRA3* (*Seita.2G396200*) encoded a trehalose-6-phosphate phosphatase (TPP), belonging to the RAMOSA (RA) gene family, and was significantly downregulated in *sifea4-8*. In maize, *RA3* functioned upstream of *RA1* together with *RA2*, positively regulating the determinacy of BM and the identity of the spikelet pair meristem (SPM). Loss of *RA3* function promoted excessive proliferation of lateral meristems, leading to increased inflorescence branching (Satoh-Nagasawa et al., 2006). *SiYABBY4* (*Seita.1G251700*) was homologous to *TONGARI-BOUSHI 1* (*OsTOB1*) of the YABBY gene family in rice, which regulated spikelet and branch meristem development (Tanaka et al., 2017). *SiAGL61* (*Seita.3G280400*) belonged to the MADS-box gene family and was homologous to *AGAMOUS-Like 61* (*AGL61*) in *Arabidopsis*, which regulated central cell development (Steffen et al., 2008). *SiBRE1B* (*Seita.1G066200*) was the homologous gene of *HISTONE MONOUBIQUITINATION1* (*OsHUB1*) associated with anther development in rice (Cao et al., 2015). By contrast, some genes related to inflorescence development were upregulated in the *sifea4-8* mutant. *SiPL3* (*Seita.5G337100*) encoded a protein containing a PLUS3 domain and was homologous to *OsPL3* in rice. *OsPL3* was a target of microRNA *OsmiR530*, and the *OsPL3* knockout mutant exhibited dwarfism, shortened panicles, small grains, and reduced number of secondary branches (Sun et al., 2020). *SiCDF1* (*Seita.9G525000*) was homologous to *OsDof12* in rice, which involved in the regulation of plant height, primary branch number, and secondary branch number (Wu et al., 2015). *SiCUC* (*Seita.7G166500*) was homologous to *CUP-SHAPED COTYLEDON1* (*CUC1*) in *Arabidopsis*, which regulated cell polarity and growth pattern (Hu et al., 2024) (Figure 5d). These results indicated that *SiFEA4* affected the expression of some genes related to inflorescence development.

Interestingly, there were no CLV and WUS-related genes in our DEGs, indicating that the *SiFEA4*-mediated regulatory pathway operated in parallel to the classical CLV-WUS negative feedback loop, which was consistent with the findings of Pautler et al. (2015) in the study of maize *FEA4*. Overall, these results suggested that *SiFEA4* regulated panicle structure through the plant hormone signaling pathway, possibly by a mechanism independent of the classical CLV-WUS negative feedback loop.

Genome-wide identification of direct downstream target genes of *SiFEA4*

To identify genome-wide binding sites of transcription factor *SiFEA4* in foxtail millet, we performed a DAP-seq experiment with two biological replicates (IP1 and IP2). A total of 23,145 binding peaks identified in IP1 and IP2 were overlapping (Figure 6a; Table S6) and primarily enriched in the cis-element "NNGATGACGTCATCN" (Motif 1), which contained the core recognition sequence (TGACG) of the TGA subfamily of the bZIP transcription factor family (Figure 6b; S4). Furthermore, 20.96% of the overlapping binding peaks located in the gene promoter regions (Figure 6c). As trans-acting factors, the transcription factors generally activated or repressed the transcription of target genes by binding to cis-acting elements in their promoter regions. Based on this, we screened genes with SiFEA4 protein binding peaks in the promoter region (-2000 bp) and enrichment fold ≥ 4 from the DAP-seq dataset (Table S7), and conducted a joint analysis with the DEGs from the RNA-seq dataset. A total of 89 potential direct downstream target genes of *SiFEA4* were identified in these two datasets, including 65 down-regulated genes and 24 up-regulated genes (Figure 6d; Table S8, S9). GO enrichment analysis of these 89 genes revealed that they were significantly enriched in biological processes such as embryo sac central cell differentiation (GO:0009559, p value = 2.43637E-02), regulation of auxin mediated signaling pathway (GO:0010928, p value = 3.63257E-02), and regulation of salicylic acid biosynthetic process (GO:0080142, p value = 4.81434E-02). In terms of molecular function, these genes were significantly enriched in GO terms such as sequence-specific DNA binding (GO:0043565, p value = 2.13795E-03), DNA-binding transcription factor activity (GO:0003700, p value = 1.39528E-02), and protein disulfide oxidoreductase activity (GO:0015035, p value = 2.23881E-02) (Figure S5; Table S10).

Studies have shown that members of the AP2/ERF transcription factor family were crucial for inflorescence branching and spikelet formation in gramineous crops, such as *FRIZZY PANICLE* (*FZP*), *OsEATB*, and *OsERF65* in rice (Komatsu et al., 2003; Qi et al., 2011; Xie et al., 2023) and *Indeterminate spikelet1* (*IDS1*) in maize (Chuck et al., 2008). *FZP* was considered as a positive regulator that promoted the transformation from BM to SM. By inhibiting the excessive proliferation of lateral meristem, FZP promoted the transformation from BM to SM and the recognition and maintenance of floral meristems. The *fzp* mutant exhibited the continuous production of primary branches and was unable to differentiate into spikelet (Komatsu et al., 2003). In maize, the AP2/ERF gene family member *IDS1* and *Branched silkless1* (*BD1*) determined the fate of SM and controlled the number of FM, and the *ids1* mutant initiated additional florets (Chuck et al., 2008; Chuck et al., 2002). In wheat and barley, the mutant of the AP2/ERF transcription factor *Compositum 2* (*COM2*) produced the spike-branching phenotype (Poursarebani et al., 2015). It was worth noting that among the 89 downstream target genes of SiFEA4 obtained through the combined analysis of DAP-seq and RNA-seq, there was a member of the AP2/ERF transcription factor

family, *Seita.6G181700* (*SiERF109*), whose promoter region had the strongest binding peak of SiFEA4 protein (Figure 6e; S6), and the binding peak was mainly enriched in the sequence "CCGCTGACGTCACCT" (belong to Motif1) containing the conserved TGACG core motif recognized by TGA transcription factors (Figure 6b, e). Futhermore, *SiERF109* was significantly downregulated in the *sifea4-8* mutant. Therefore, we speculated that *SiFEA4* might directly target *SiERF109* to regulate the inflorescence development in foxtail millet. In addition, among the 89 downstream target genes of SiFEA4, there were also genes such as *SiCDF1*, *SiAGL61* and *SiPL3* (Figure S6), which were related to inflorescence development. For *SiCDF1*, the SiFEA4 protein binding peaks were mainly enriched in the sequence "TGCTGATGTCATCC" within its promoter region, which corresponded to the Motif 1 (Figure 6b, f). There were multiple binding peaks of SiFEA4 protein in the promoter region of *SiAGL61*. Among them, the most confident motif was Motif 15, whose corresponding sequence was "TCGTCATACT", and this sequence was far from the transcription start site (TSS) (Figure 6g-h). In *SiPL3*, the binding peaks of SiFEA4 were mainly enriched in the sequence "GACGGGACG" within its promoter region, which belonged to Motif17 (Figure 6i-j). However, the fold enrichment of SiFEA protein binding to the promoters of these three genes, as well as the differential expression ratio, were significantly lower than those of *SiERF109* (Figure S6).

Discussion

The functions of *SiFEA4* and its homologs in the regulation of IM size and inflorescence development were conserved.

In this study, through map-based cloning and CRISPR-Cas9 mediated gene knockout function validation, we identified *SiFEA4* as a gene controlling the panicle apex branching in foxtail millet, which encoded a bZIP transcription factor (Figure 2 and 4). Phylogenetic analysis revealed that *SiFEA4* was highly homologous to the previously reported genes related to inflorescence development, such as *FEA4*, *HvFEA4*, *PAN*, and *OsbZIP47* (Figure S2). In maize, the *fea4* mutant exhibited the enlarged IM size and IM apical flattening at early developmental stages, leading to the thicker tassel main axis with higher spikelet density, severely flattened ear with shortened ear length, disorganized kernel arrangement, increased kernel row number, and branching at the tips of the ear (Pautler et al., 2015). In barley, the *hvfea4* mutant showed the enlarged IM, ectopic spikelets on the rachis, but shortened spike and reduced spikelet number, ultimately resulting in the decreased yield (Wang et al., 2023). In rice, the *OsbZIP47* knockout mutant exhibited the reduced plant height, enlarged meristems, delayed flowering, increased stamen number, and wider grains (Prakash et al., 2022). Moreover, in the dicot plant *Arabidopsis*, the *pan* mutant displayed the increased floral organ number and enlarged SAM (Running et al., 1996; Chuang et al., 1999; Maier et al., 2011). In this study, the *sifea4* mutant showed the enlarged and abnormally flattened IM, leading to the panicle apex branching, ectopic panicle primary branches on the rachis, and slender panicle primary branches (Figure 4), which were highly similar to the phenotype of its homologous gene mutant. These findings strongly suggested that *SiFEA4* and its orthologs were not only highly similar in sequence, but also highly conserved in regulating meristem size and inflorescence development in monocot and dicot plants.

Molecular network analysis of *SiFEA4* regulating inflorescence development in foxtail millet

Transcriptome analysis revealed that *SiFEA4* regulated inflorescence development by the plant hormone signaling pathway, including jasmonic acid, abscisic acid, gibberellin, and ethylene (Figure 5; Table S5). This finding was highly consistent with the study on rice *OsbZIP47*, which also regulated hormone signaling pathway (Prakash et al., 2022). Notably, multiple DEGs associated with inflorescence development and plant hormones identified in this study largely overlapped with the research results of Pautler et al. (2015), which identified DEGs between maize wild-type and *fea4* mutant. These overlapped genes included the RAMOSA family gene regulating inflorescence branching, CUC gene controlling organ initiation and boundary formation, and genes encoding auxin early response proteins. Interestingly, no DEGs related to CLV and WUS were identified in this study (Table S4), suggesting that *SiFEA4* regulated inflorescence development independently of the CLV-WUS negative feedback pathway, which was similar to that of the *FEA4* in maize (Pautler et al., 2015).

In the present study, 23,145 binding peaks of SiFEA4 were identified throughout the genome using DAP-seq (Figure 6; Table S6). These binding peaks were predominantly enriched in the conserved "TGACGTCA" motif (Figure S4), which contained the core sequence "TGACG" recognized by TGA transcription factors (Katagiri et al., 1989), validating the reliability of the DAP-seq data. Studies have shown that AP2/ERF family genes were core regulators of panicle branching and spikelet fate in grasses, for example, the gene *FZP*, *OsEATB*, and *OsERF65* in rice; the gene *IDS1* and *BD1* in maize; and the gene *COM2* in wheat. They all determined panicle branching and spikelet determinacy (Komatsu et al., 2003; Qi et al., 2011; Xie et al., 2023; Chuck et al., 2008; Chuck et al., 2002; Poursarebani et al., 2015). Through integrated analysis of DAP-seq and RNA-seq, this study identified 89 potential downstream target genes of *SiFEA4*. Among them, the AP2/ERF family gene *SiERF109* exhibited the strongest binding peak of SiFEA4 in its promoter region, and its expression level was significantly downregulated in the mutant. Therefore, we hypothesized that SiFEA4 might directly target *SiERF109* to regulate inflorescence development in foxtail millet. Additionally, other inflorescence development-related genes, such as *SiCDF1*, *SiPL3*, and *SiAGL61*, were also identified as potential targets of *SiFEA4*. However, these findings still needed to be further verified through molecular biological techniques such as yeast one-hybrid and EMSA, as well as genetic experiments.

Analysis of the potential breeding utilization value of *SiFEA4*

The panicle primary branches of foxtail millet growed on the panicle axis, and the panicle included primary, secondary, and tertiary branches, with spikelets and bristles attached to the tertiary branches, and the fertile florets within the spikelets eventually developed into grains. Therefore, the number of panicle primary branches, spikelets, and fertile florets collectively determined the grain number per panicle in foxtail millet, thereby affecting the yield. Zhang et al. (2022) overexpressed a specific allele of *TaCOL-B5* in common wheat, which regulated spikelets number, leading to an increase in spikelets number and, in turn, grain yield per spike. In this study, loss-of-function mutants of *SiFEA4* produced extra panicle primary branches on the rachis, similar to the ectopic spikelet phenotype of *hvfea4* (Wang

et al., 2023), resulting in 54.29% and 46.57% increase in the number of panicle primary branches in the *sifea4-8* and *sifea4-9* mutant, respectively (Figure 4f and m). Although the number of panicle primary branches increased significantly, the structure of the panicle primary branches became slender and the number of grains per panicle primary branch reduced 40.52% and 42.51% in the *sifea4*-8 and *sifea4*-9 mutant, respectively, ultimately resulting in no significant change in panicle weight (Figure 4j and m-p). This was similar to the finding of Lu et al. (2026), which showed that excessive increase in spikelets would lead to a decrease in the number of grains. The slender shape of the panicle primary branches might result from the over-proliferation of panicle primary branches on the rachis, which excessively compressed the rachis space, thereby inhibiting the lateral development of the panicle primary branches while promoting longitudinal growth, ultimately forming the relatively slender panicle primary branches. Studies have shown that weak alleles of some genes related to the meristem development could increase yield. For example, the weak alleles of the maize *FEA2* and *FEA3* genes increased ear length, kernel row number and kernels number per ear (Bommert et al., 2013; Je et al., 2016). Therefore, using the CRISPR systerm to precisely regulate *SiFEA4* expression (e.g., by targeting cis-regulatory elements in its promoter) and generate germplasm with weak allele of *SiFEA4* may achieve a balance between the number and the structure of panicle primary branches, fully utilize rachis space, and thus increase grain yield per panicle in foxtail millet. Notably, unlike the significantly shortened ear/panicle length observed in maize *fea4*, barley *hvfea4*, and rice *osbzip47* mutants, the panicle length of the *sifea4* mutants did not change significantly, but they all showed the reduced plant height. This not only highlighted the potential of *SiFEA4* for panicle architecture improvement but also suggested that *SiFEA4* and its orthologs were highly functionally conserved in regulating plant height in cereal crops, providing an important breeding target for reducing plant height in foxtail millet (Pautler et al., 2015; Wang et al., 2023; Prakash et al., 2022).

In summary, this study identified the bZIP transcription factor *SiFEA4* controlling the panicle apex branching in foxtail millet through map-based cloning. *SiFEA4* was a pleiotropic gene that not only regulated the panicle apical branching phenotype but also participated in controlling plant height and the number and structure of panicle primary branches. RNA-seq revealed that *SiFEA4* regulated panicle development likely through the plant hormone signaling pathway. Additionally, integrated analysis of DAP-seq and RNA-seq identified the 89 potential direct downstream target genes of *SiFEA4*, including *SiERF109*, *SiCDF1*, *SiPL3*, and *SiAGL61*. These findings provided a novel insight into understanding panicle architecture development and offered new target for genetic improvement of panicle architecture in foxtail millet.

Declarations

Author contribution

GHY, LLG, JGW, and XYY designed the experiments. GHY, LLG, and TGW performed experiments. LC, SKN, YYY, SJD, YQZ, SYW, YXM, and LJY collected the phenotype. LLG and TGW wrote the manuscript.

KZ, XRL, SQD, HZW and XQC helped revise the manuscript. All authors reviewed and approved the final manuscript.

Funding

This work was supported by Fundamental Research Program of Shanxi Province (202203021222169, 20210302123382), Special Plan for Scientific and Technological Innovation Talent Team of Shanxi Province (202204051002036), Shanxi Agricultural University Doctoral Research Initiation Project (2021BQ23, 2021BQ24) and Award Scientific Program for Excellent Doctors in Shanxi Province (SXBYKY2021070, SXBYKY2021059).

Conflict of interest

The authors declare that they have no conflict of interest.

Data Availability Statement

All data are presented in the manuscript and figures, with additional supporting information provided in the Supplementary Information.

References

1. Bartlett, A., O'Malley, R.C., Huang, S.C., Galli, M., Nery, J.R., Gallavotti, A. et al. (2017) Mapping genome-wide transcription-factor binding sites using DAP-seq. *Nature Protocols*, 12, 1659-1672. https://doi.org/10.1038/nprot.2017.055
2. Bennetzen, J.L., Schmutz, J., Wang, H., Percifield, R., Hawkins, J., Pontaroli, A.C. et al. (2012) Reference genome sequence of the model plant *Setaria*. *Nature Biotechnology*, 30, 555-561. https://doi.org/10.1038/nbt.2196
3. Bettinger, R.L., Barton, L. & Morgan, C. (2010) The origins of food production in north China: A different kind of agricultural revolution. *Evolutionary Anthropology*, 19, 9-21. https://doi.org/10.1002/evan.20236
4. Bommert, P., Lunde, C., Nardmann, J., Vollbrecht, E., Running, M., Jackson, D. et al. (2005) *thick tassel dwarf1* encodes a putative maize ortholog of the *Arabidopsis* CLAVATA1 leucine-rich repeat receptor-like kinase. *Development*, 132, 1235-1245. https://doi.org/10.1242/dev.01671
5. Bommert, P., Nagasawa, N.S. & Jackson, D. (2013) Quantitative variation in maize kernel row number is controlled by the *FASCIATED EAR2* locus. *Nature Genetics*, 45, 334-337. https://doi.org/10.1038/ng.2534
6. Brand, U., Fletcher, J.C., Hobe, M., Meyerowitz, E.M. & Simon, R. (2000) Dependence of stem cell fate in *Arabidopsis* on a feedback loop regulated by CLV3 activity. *Science*, 289, 617-619. https://doi.org/10.1126/science.289.5479.617

7. Cao, H., Li, X., Wang, Z., Ding, M., Sun, Y., Dong, F. et al. (2015) Histone H2B monoubiquitination mediated by HISTONE MONOUBIQUITINATION1 and HISTONE MONOUBIQUITINATION2 is involved in anther development by regulating tapetum degradation-related genes in rice. *Plant Physiology*, 168, 1389-1405. https://doi.org/10.1104/pp.114.256578
8. Chu, H., Qian, Q., Liang, W., Yin, C., Tan, H., Yao, X. et al. (2006) The *floral organ number4* gene encoding a putative ortholog of *Arabidopsis CLAVATA3* regulates apical meristem size in rice. *Plant Physiology*, 142, 1039-1052. https://doi.org/10.1104/pp.106.086736
9. Chuang, C.F., Running, M.P., Williams, R.W. & Meyerowitz, E.M. (1999) The *PERIANTHIA* gene encodes a bZIP protein involved in the determination of floral organ number in *Arabidopsis thaliana*. *Genes & Development*, 13, 334-344. https://doi.org/10.1101/gad.13.3.334
10. Chuck, G., Meeley, R. & Hake, S. (2008) Floral meristem initiation and meristem cell fate are regulated by the maize AP2 genes *ids1* and *sid1*. *Development*, 135, 3013-3019. https://doi.org/10.1242/dev.024273
11. Chuck, G., Muszynski, M., Kellogg, E., Hake, S. & Schmidt, R.J. (2002) The control of spikelet meristem identity by the *branched silkless1* gene in maize. *Science*, 298, 1238-1241. https://doi.org/10.1126/science.1076920
12. Clark, S.E., Williams, R.W. & Meyerowitz, E.M. (1997) The *CLAVATA1* gene encodes a putative receptor kinase that controls shoot and floral meristem size in *Arabidopsis*. *Cell*, 89, 575-585. https://doi.org/10.1016/s0092-8674(00)80239-1
13. Fletcher, J.C., Brand, U., Running, M.P., Simon, R. & Meyerowitz, E.M. (1999) Signaling of cell fate decisions by CLAVATA3 in *Arabidopsis* shoot meristems. *Science*, 283, 1911-1914. https://doi.org/10.1126/science.283.5409.1911
14. Hu, Z.-L., Wilson-Sánchez, D., Bhatia, N., Rast-Somssich, M.I., Wu, A., Vlad, D. et al. (2024) A CUC1/auxin genetic module links cell polarity to patterned tissue growth and leaf shape diversity in crucifer plants. *Proceedings of the National Academy of Sciences*, 121, e2321877121. https://doi.org/10.1073/pnas.2321877121
15. Je, B.I., Gruel, J., Lee, Y.K., Bommert, P., Arevalo, E.D., Eveland, A.L. et al. (2016) Signaling from maize organ primordia via *FASCIATED EAR3* regulates stem cell proliferation and yield traits. *Nature Genetics*, 48, 785-791. https://doi.org/10.1038/ng.3567
16. Je, B.I., Xu, F., Wu, Q., Liu, L., Meeley, R., Gallagher, J.P. et al. (2018) The CLAVATA receptor FASCIATED EAR2 responds to distinct CLE peptides by signaling through two downstream effectors. *eLife*, 7, e35673. https://doi.org/10.7554/eLife.35673
17. Jeong, S., Trotochaud, A.E. & Clark, S.E. (1999) The *Arabidopsis CLAVATA2* gene encodes a receptor-like protein required for the stability of the CLAVATA1 receptor-like kinase. *The Plant Cell*, 11, 1925-1933. https://doi.org/10.1105/tpc.11.10.1925
18. Katagiri, F., Lam, E. & Chua, N.H. (1989) Two tobacco DNA-binding proteins with homology to the nuclear factor CREB. *Nature*, 340, 727-730. https://doi.org/10.1038/340727a0

19. Komatsu, M., Chujo, A., Nagato, Y., Shimamoto, K. & Kyozuka, J. (2003) *FRIZZY PANICLE* is required to prevent the formation of axillary meristems and to establish floral meristem identity in rice spikelets. *Development*, 130, 3841-3850. https://doi.org/10.1242/dev.00564
20. Lu, R., Zheng, S., Yang, L., Li, Z., Si, Y., Yan, M. et al. (2026) Image-based rachis phenotyping facilitates genetic dissection of spikelet distribution in wheat. *Plant Physiology*, 200, kiaf666. https://doi.org/10.1093/plphys/kiaf666
21. Maier, A.T., Stehling-Sun, S., Offenburger, S.L. & Lohmann, J.U. (2011) The bZIP transcription factor *PERIANTHIA*: a multifunctional hub for meristem control. *Frontiers in Plant Science*, 2, 79. https://doi.org/10.3389/fpls.2011.00079
22. Pautler, M., Eveland, A.L., LaRue, T., Yang, F., Weeks, R., Lunde, C. et al. (2015) *FASCIATED EAR4* encodes a bZIP transcription factor that regulates shoot meristem size in maize. *The Plant Cell*, 27, 104-120. https://doi.org/10.1105/tpc.114.132506
23. Poursarebani, N., Seidensticker, T., Koppolu, R., Trautewig, C., Gawroński, P., Bini, F. et al. (2015) The genetic basis of composite spike form in barley and 'Miracle-Wheat'. *Genetics*, 201, 155-165. https://doi.org/10.1534/genetics.115.176628
24. Prakash, S., Rai, R., Zamzam, M., Ahmad, O., Peesapati, R. & Vijayraghavan, U. (2022) *OsbZIP47* is an integrator for meristem regulators during rice plant growth and development. *Frontiers in Plant Science*, 13, 865928. https://doi.org/10.3389/fpls.2022.865928
25. Qi, W., Sun, F., Wang, Q., Chen, M., Huang, Y., Feng, Y.Q. et al. (2011) Rice ethylene-response AP2/ERF factor *OsEATB* restricts internode elongation by down-regulating a gibberellin biosynthetic gene. *Plant Physiology*, 157, 216-228. https://doi.org/10.1104/pp.111.179945
26. Running, M.P. & Meyerowitz, E.M. (1996) Mutations in the *PERIANTHIA* gene of *Arabidopsis* specifically alter floral organ number and initiation pattern. *Development*, 122, 1261-1269. https://doi.org/10.1242/dev.122.4.1261
27. Satoh-Nagasawa, N., Nagasawa, N., Malcomber, S.T., Sakai, H. & Jackson, D. (2006) A trehalose metabolic enzyme controls inflorescence architecture in maize. *Nature*, 441, 227-230. https://doi.org/10.1038/nature04725
28. Schoof, H., Lenhard, M., Haecker, A., Mayer, K.F.X., Jürgens, G. & Laux, T. (2000) The stem cell population of *Arabidopsis* shoot meristems is maintained by a regulatory loop between the *CLAVATA* and *WUSCHEL* genes. *Cell*, 100, 635-644. https://doi.org/10.1016/S0092-8674(00)80700-X
29. Steffen, J.G., Kang, I.H., Portereiko, M.F., Lloyd, A. & Drews, G.N. (2008) AGL61 interacts with AGL80 and is required for central cell development in *Arabidopsis*. *Plant Physiology*, 148, 259-268. https://doi.org/10.1104/pp.108.119404
30. Sun, W., Xu, X.H., Li, Y., Xie, L., He, Y., Li, W. et al. (2020) OsmiR530 acts downstream of *OsPIL15* to regulate grain yield in rice. *New Phytologist*, 226, 823-837. https://doi.org/10.1111/nph.16399
31. Suzaki, T., Sato, M., Ashikari, M., Miyoshi, M., Nagato, Y. & Hirano, H.-Y. (2004) The gene *FLORAL ORGAN NUMBER1* regulates floral meristem size in rice and encodes a leucine-rich repeat receptor

kinase orthologous to *Arabidopsis* CLAVATA1. *Development*, 131, 5649-5657. https://doi.org/10.1242/dev.01441

32. Suzaki, T., Toriba, T., Fujimoto, M., Tsutsumi, N., Kitano, H. & Hirano, H.Y. (2006) Conservation and diversification of meristem maintenance mechanism in *Oryza sativa*: function of the *FLORAL ORGAN NUMBER2* gene. *Plant and Cell Physiology*, 47, 1591-1602. https://doi.org/10.1093/pcp/pcl025
33. Taguchi-Shiobara, F., Yuan, Z., Hake, S. & Jackson, D. (2001) The *fasciated ear2* gene encodes a leucine-rich repeat receptor-like protein that regulates shoot meristem proliferation in maize. *Genes & Development*, 15, 2755-2766. https://doi.org/10.1101/gad.208501
34. Tanaka, W., Pautler, M., Jackson, D. & Hirano, H.Y. (2013) Grass meristems II: inflorescence architecture, flower development and meristem fate. *Plant and Cell Physiology*, 54, 313-324. https://doi.org/10.1093/pcp/pct016
35. Tanaka, W., Toriba, T. & Hirano, H.Y. (2017) Three TOB1-related YABBY genes are required to maintain proper function of the spikelet and branch meristems in rice. *New Phytologist*, 215, 825-839. https://doi.org/10.1111/nph.14617
36. Vidhya, C.S., Girase, I.P., Spandana, B., Jejal, A.D., Singh, M., Karmakar, A. et al. (2023) Enhancing nutritional security and combating hidden hunger with climate-resilient millets. *International Journal of Environment and Climate Change*, 13, 4587-4602. https://doi.org/10.9734/IJECC/2023/v13i113638
37. Wang, C., Yang, X. & Li, G. (2021) Molecular insights into inflorescence meristem specification for yield potential in cereal crops. *International Journal of Molecular Sciences*, 22, 3508. https://doi.org/10.3390/ijms22073508
38. Wang, C., Yang, X., Zhang, Y., Shen, C., Shi, J., Xia, C. et al. (2023) Barley *FASCIATED EAR* genes determine inflorescence meristem size and yield traits. *The Crop Journal*, 11, 679-691. https://doi.org/10.1016/j.cj.2022.10.001
39. Wu, Q., Li, D., Li, D., Liu, X., Zhao, X. & Li, X. (2015) Overexpression of *OsDof12* affects plant architecture in rice (*Oryza sativa L.*). *Frontiers in Plant Science*, 6, 833. https://doi.org/10.3389/fpls.2015.00833
40. Xie, W., Cao, W., Lu, S., Zhao, J., Shi, X., Yue, X. et al. (2023) Knockout of transcription factor *OsERF65* enhances ROS scavenging ability and confers resistance to rice sheath blight. *Molecular Plant Pathology*, 24, 1535-1551. https://doi.org/10.1111/mpp.13391
41. Xing, H.-L., Dong, L., Wang, Z.-P., Zhang, H.-Y., Han, C.-Y., Liu, B. et al. (2014) A CRISPR/Cas9 toolkit for multiplex genome editing in plants. *BMC Plant Biology,* 14, 327. https://doi.org/10.1186/s12870-014-0327-y
42. Yang, X., Wan, Z., Perry, L., Lu, H., Wang, Q., Zhao, C. et al. (2012) Early millet use in northern China. *Proceedings of the National Academy of Sciences*, 109, 3726-3730. https://doi.org/10.1073/pnas.1115430109
43. Zepeda, B. & Verdonk, J.C. (2022) RNA extraction from plant tissue with homemade acid guanidinium thiocyanate phenol chloroform (AGPC). *Current Protocols*, 2, e351.

https://doi.org/10.1002/cpz1.351

44. Zhang, X., Jia, H., Li, T., Wu, J., Nagarajan, R., Lei, L. et al. (2022) *TaCol-B5* modifies spike architecture and enhances grain yield in wheat. *Science*, 376, 180-183. https://doi.org/10.1126/science.abm0717
45. Zhu, C., Liu, L., Crowell, O., Zhao, H., Brutnell, T.P., Jackson, D. et al. (2021) The CLV3 homolog in *Setaria viridis* selectively controls inflorescence meristem size. *Frontiers in Plant Science*, 12, 636749. https://doi.org/10.3389/fpls.2021.636749

Figures

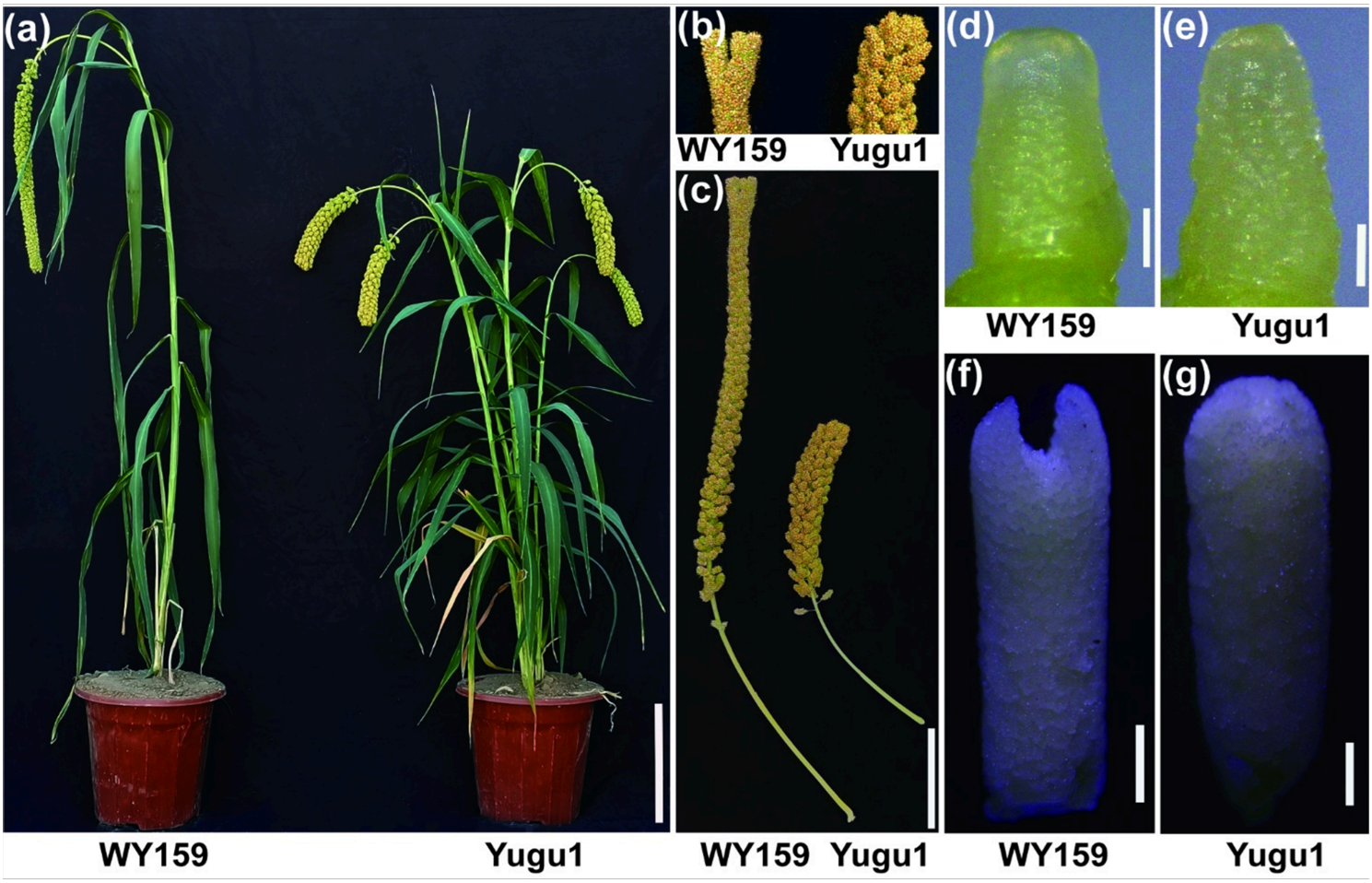


Figure 1

Identification of the panicle apex branching trait in Foxtail Millet. (a) Comparison of the whole plant between WY159 and Yugu1. Scale bar = 20 cm. (b) The enlarged image of the top of the panicle in (c). (c) Comparison of the panicle between WY159 and Yugu1. Scale bar = 10 cm. The IM of WY159 (d) and Yugu1 (e) at the stage of IM to BM transition. Scale bar = 200 μm. The young panicle of WY159 (f) and Yugu1 (g). Scale bar = 1 mm.

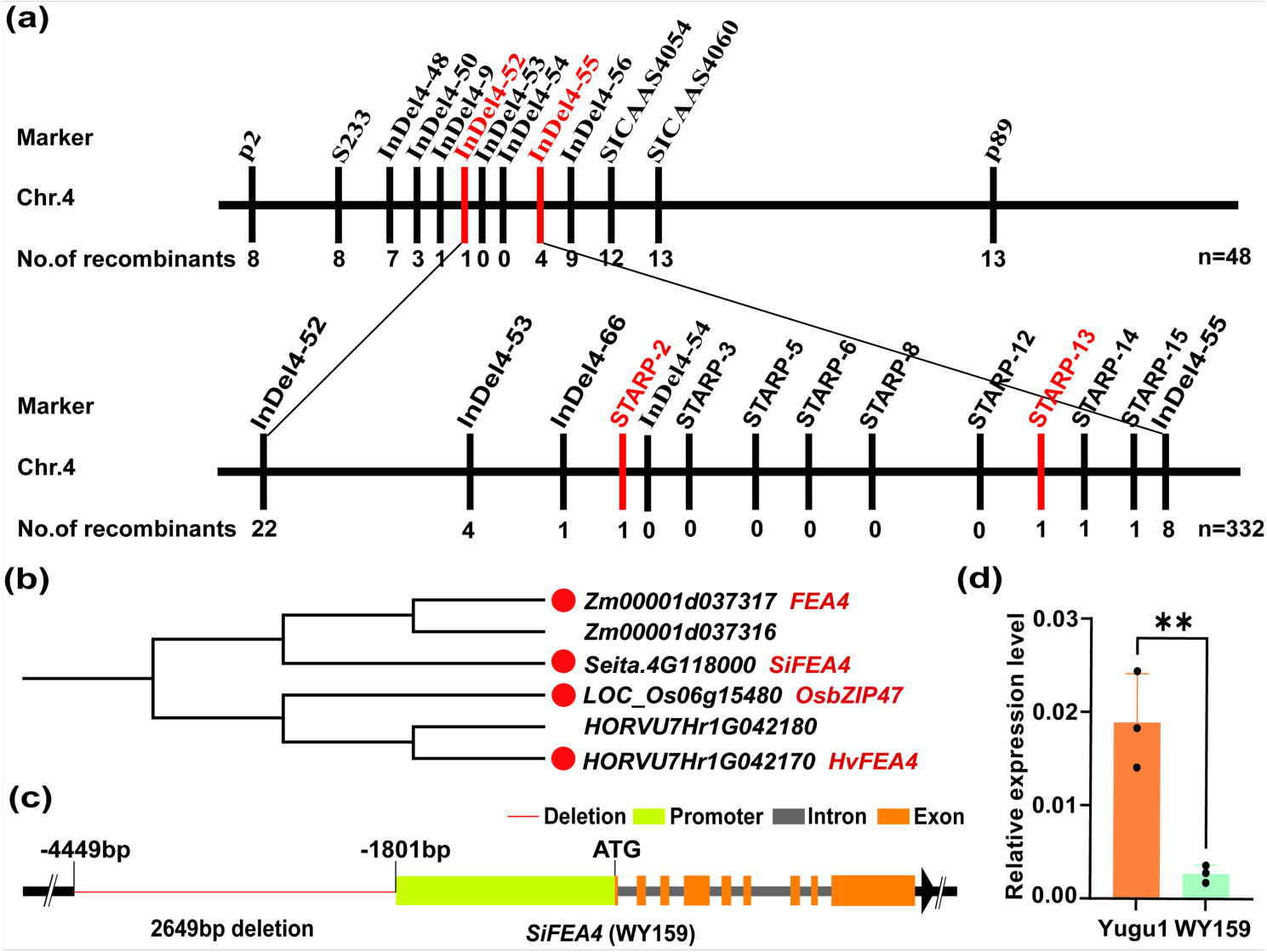


Figure 2

Map-based cloning and candidate gene analysis. (a) Map-based cloning of the panicle apex branching gene in foxtail millet. (b) Partial phylogenetic analysis of SiFEA4 and its homologous proteins. (c) Compared to Yugu1, the *SiFEA4* exhibited a 2649-bp deletion in the promoter region in WY159. (d) Relative expression of *SiFEA4* in young panicle of Yugu1 and WY159. Data were presented as means ± standard deviation. **P < 0.01 (Student's t-test).

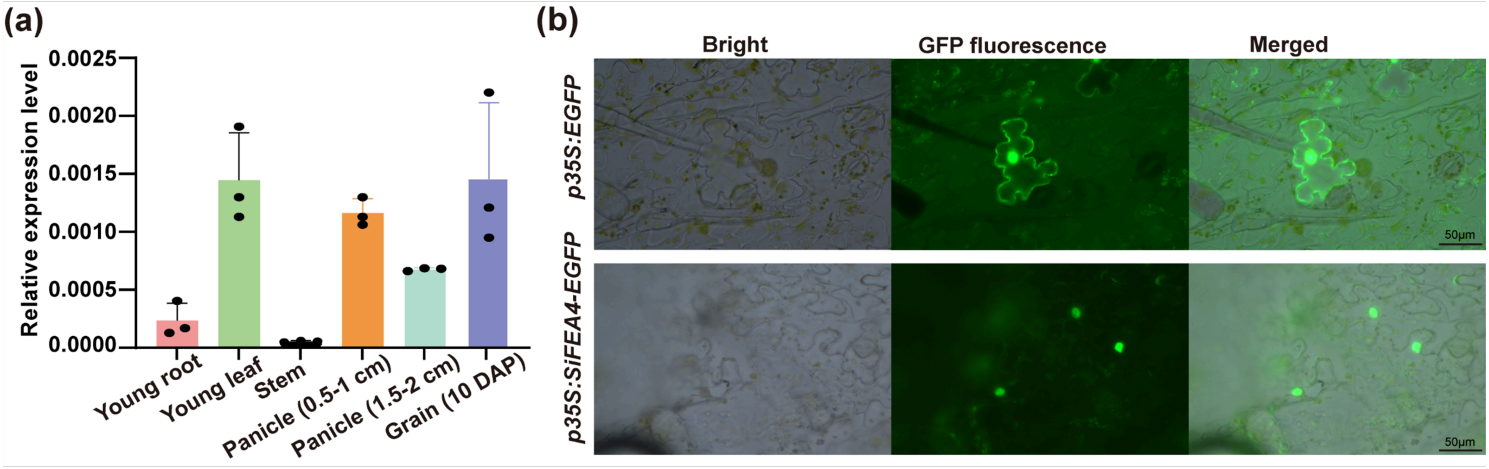


Figure 3

The expression pattern and protein subcellular localization of *SiFEA4*. (a) Relative expression of *SiFEA4* in various tissues of Yugu1. Data were presented as means ± standard deviation. (b) Subcellular localization of the SiFEA4 protein in the epidermal cells of tobacco leaves.

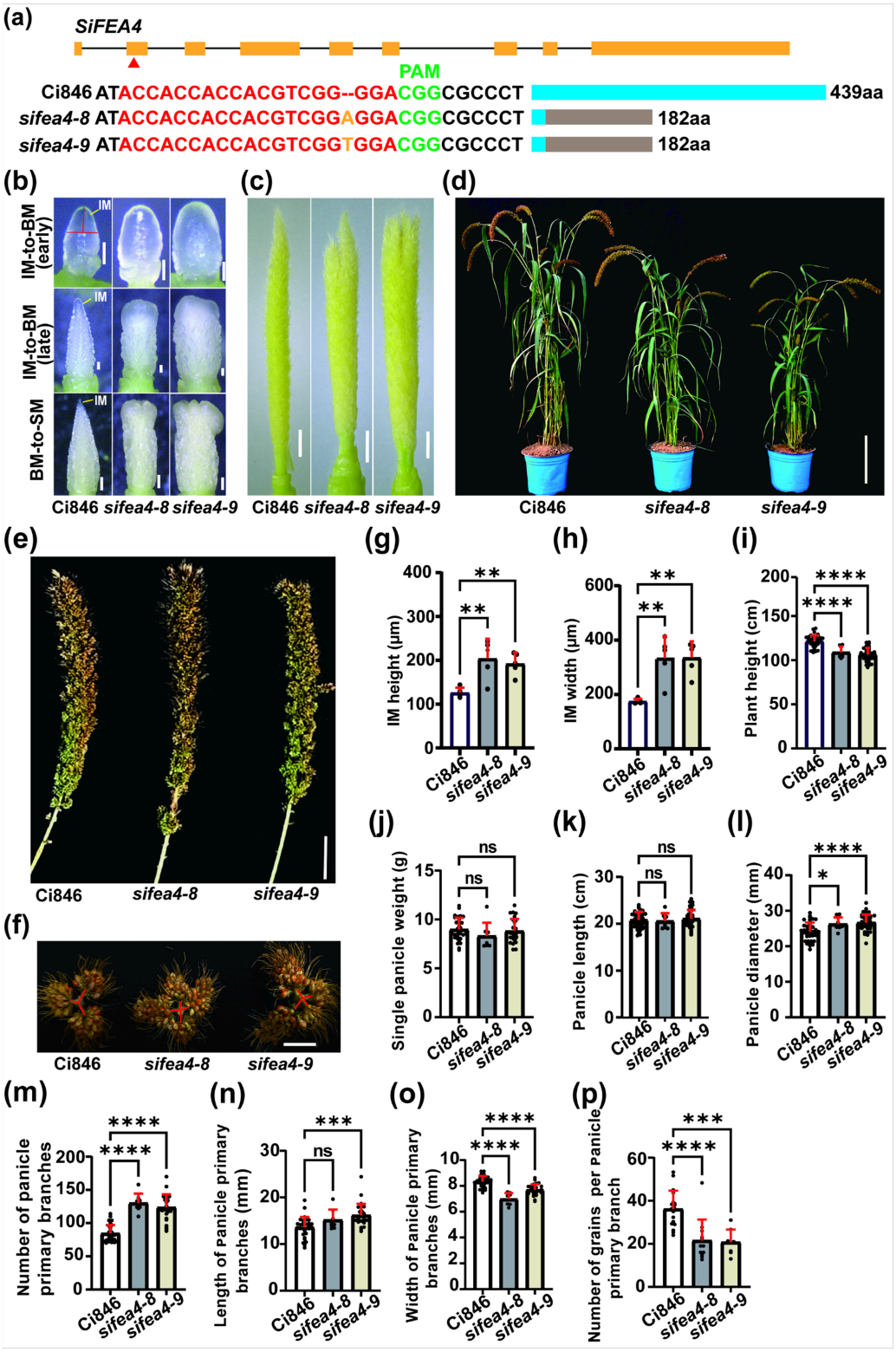


Figure 4

Verification of *SiFEA4* function by the CRISPR/Cas9-mediated knockout in foxtail millet. (a) The mutation sites of two homozygous knockout lines (*sifea4-8* and *sifea4-9*). (b) Phenotypic comparison of the early inflorescence of Ci846, *sifea4-8* and *sifea4-9*. The red horizontal and vertical line represented the position where the width and height of IM was measured, respectively. Scale bars at the IM-to-BM stage = 100 μm. Scale bars at BM-to-SM stage = 500 μm. (c) The young panicle phenotypes of Ci846, *sifea4-8* and

sifea4-9. Scale bars = 2 mm. (d) The overall plant morphology of Ci846, *sifea4-8* and *sifea4-9*. Scale bars = 20 cm. (e) The panicle phenotype of Ci846, *sifea4-8* and *sifea4-9*. Scale bars = 5 cm. (f) Compare with Ci846, *sifea4-8* and *sifea4-9*developed extra panicle primary branches. Scale bar = 1 cm. Statistical analysis of the IM height (g), IM width (h), plant height (i), single panicle weight (j), panicle length (k), panicle diameter (l), number of panicle primary branches (m), length of panicle primary branches (n), width of panicle primary branches (o), and number of grains per panicle primary branch (p) of Ci846, *sifea4-8*and *sifea4-9*. Data were presented as means ± standard deviation. 'ns' indicated no significant difference. *P < 0.05, **P < 0.01, ***P < 0.001, ****P < 0.0001 (Student's t-test).

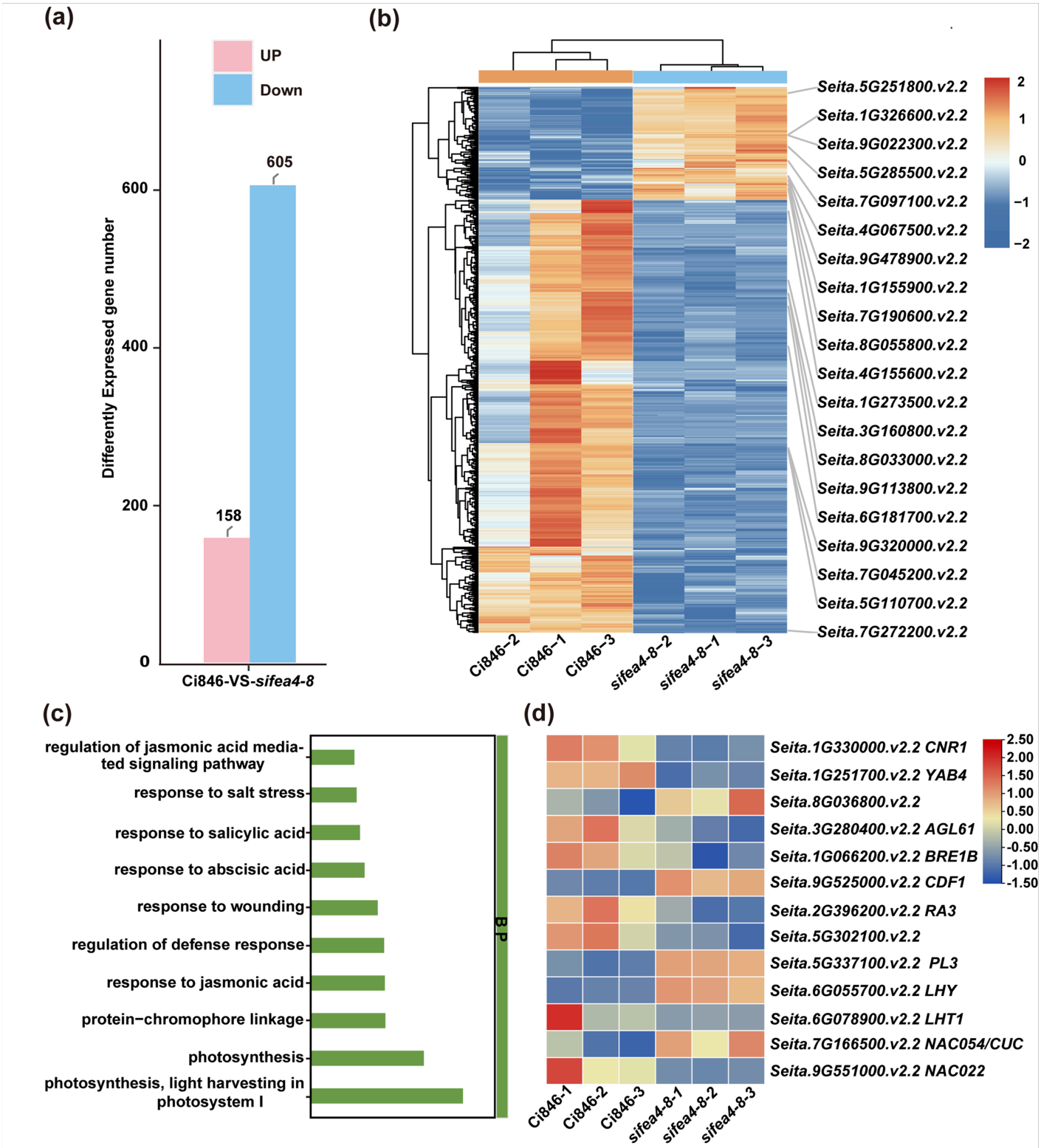


Figure 5

Transcriptome analysis of Ci846 and *sifea4-8*. (a) Statistical diagram of the DEGs between Ci846 and *sifea4-8*. (b) Heatmap of DEGs, with the top 20 DEGs displayed on the right side of the heatmap. (c) The top 10 GO terms in the biological process category of the GO enrichment analysis. (d) Heatmap of DEGs associated with inflorescence development.

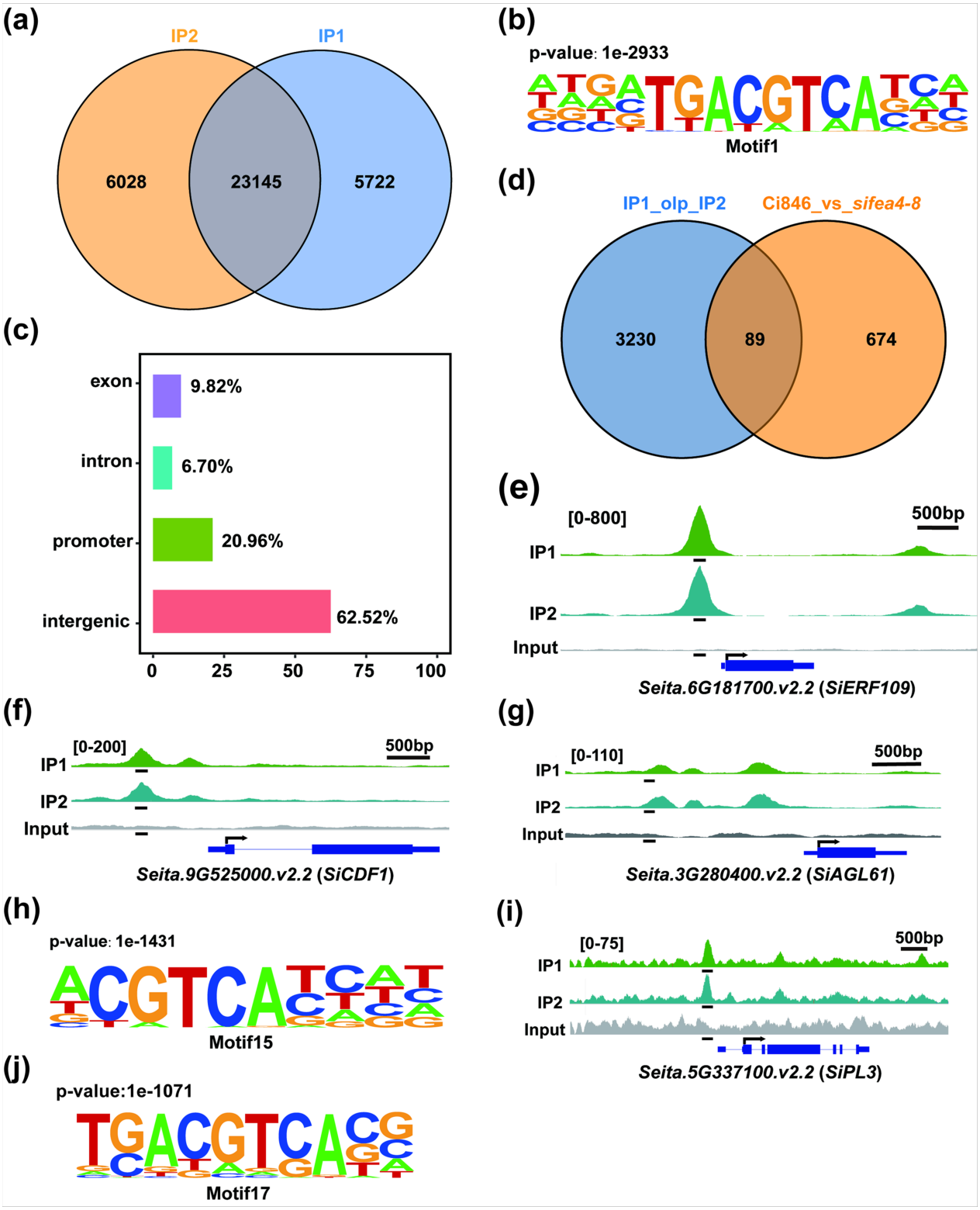


Figure 6

Identification of the direct downstream target genes of *SiFEA4*. (a) Venn diagram of overlapping binding peaks of the two biological replicates (IP1 and IP2) in DAP-seq. (b) The motif with the highest binding confidence to SiFEA4 protein in DAP-seq. (c) Genomic distribution of the overlapping binding peaks shared by the two replicates of DAP-seq. (d) Venn diagram showed the shared 89 genes between genes with overlapping binding peaks (fold enrichment ≥ 4) in promoter regions from DAP-seq data and DEGs

from RNA-seq data. The binding sites of the SiFEA4 protein in the promoters of *SiERF109* (e), *SiCDF1* (f), *SiAGL61* (g),and *SiPL3* (i). The motifs with the highest binding confidence to the SiFEA4 protein in the promoter regions of *SiAGL61* (h) and *SiPL3* (j).

Supplementary Files

This is a list of supplementary files associated with this preprint. Click to download.

- FigureS1.tiff
- FigureS2.tiff
- FigureS3.tiff
- FigureS4.tiff
- FigureS5.tiff
- FigureS6.tiff
- TableS110.xlsx